5-2008

Computational Modeling of Oxidative Stress: an Analysis of NAD (P)H Effects on Nitric Oxide and Superoxide During Hypertension

Aaron Strobel
University of Arkansas, Fayetteville

Computational Modeling of Oxidative Stress: An Analysis of NAD(P)H effects on Nitric Oxide and Superoxide during Hypertension.

Aaron Strobel

Undergraduate Honors Thesis
Dr. Mahendra Kavdia
Biological Engineering Department
University of Arkansas

Spring 2008

Committee:
Dr. Mahendra Kavdia
Dr. Tom Costello
Dr. Sreekala Bajwa

Abstract

Nitric oxide (NO) is inactivated in the human body when exposed to superoxide (O_2^-). This reaction forms peroxynitrite ($ONOO^-$). Superoxide is produced in the cardiac system by several different ways, including NAD(P)H oxidase. Superoxide dismutase (SOD) breaks down superoxide into oxygen and hydrogen peroxide. This prevents superoxide from reacting with nitric oxide and allows normal function to take place. Superoxide and peroxynitrite are main contributors to vascular disease in the human body, in particular hypertension. Experiments have shown that there was an increase of superoxide production in spontaneously hypertensive rats (SHR) vs. age-matched Wistar Kyoto rats (WKY) that were normotensive. The increase in superoxide production intensified in the presence of scavenger DETCA Cu^{2+}/Zn^{2+}. A mathematical model has been developed by Kavdia and Popel to calculate concentrations of NO, $ONOO^-$, and O_2^- in the arterial and venule pair. Using this model we calculated the arterial and venule NO, $ONOO^-$, and O_2^- concentration profiles for normotension, hypertension, SOD inactivation, and NAD(P)H stimulated cases, and analyzed which specific regions showed amplification or reductions in concentrations. The inactivation of SOD allowed O_2^- concentration to significantly increase by 10-fold under basal conditions in hypertensive mice, while reducing the NO concentration in the model. Basilar arteries from hypertensive rats showed an increase of 4.1-fold in Nox4 compared to normotensive rats. The results suggest that the increase in superoxide in hypertensive rats is in correlation with the increase of NAD(P)H oxidase in these rats. The trends in superoxide production in this paper can help understand hypertension and vascular disease more thoroughly. Further, the increase of Nox1 and Nox4 expression suggested, for future research, the specific regions where O_2^- will be high and needs to be evaluated.

Introduction

Cardiovascular disease is the leading cause of death in the United States. According to the American Heart Association, this disease was responsible for taking over 870,000 lives in 2005 in the United States. Increased vascular production of reactive oxygen species (ROS) is a common characteristic of cardiovascular disease[5]. There are several factors that increase the risk of cardiovascular disease including hypertension, hypercholesterolemia, and diabetes mellitus[6]. In the United States, hypertension affects approximately 58 million Americans.

Vascular and cardiac tissues are rich sources of ROS, including superoxide (O_2^-), hydrogen peroxide (H_2O_2), and peroxynitrite ($ONOO^-$) [7]. Reactive oxygen species are the by-products of oxygen metabolism and are normally present in low levels of concentration inside the cells[8]. ROS are needed in aiding the signaling processes within the cells, and also in regulating vascular smooth muscle cell contraction and relaxation. Increasing amounts of O_2^- is the most common trend in vascular diseases, such as hypertension, because it causes oxidative stress in the vascular tissue[9]. One of the mechanisms for controlling oxidative stress in the vascular system is superoxide dismutase. Superoxide dismutase consumes O_2^-, and then converts it into less harmful compounds[10].

The major sources of vascular superoxide include xanthine oxidase, nitric oxide synthases, mitochondrial oxidases, or NAD(P)H oxidases[11]. Each of these sources generates superoxide in a different mannerism in the human body.

Xanthine oxidase (XO) is a iron sulfur flavoprotein that is found in high concentrations in the endothelial cells and plasma, but not in smooth muscle cells[12]. Xanthine generates the superoxide by catalyzing hypoanthine and xanthine to form uric acid.

Nitric oxidase synthases (NOS), found predominantly in the endothelial cell region, play a major role in vascular diseases. Endothelial nitric oxidase synthases (eNOS) requires tetrahydrobiopterin (BH_4) for the transfer of electrons to the nitrone of the L-arginine[12]. This reaction under normal conditions forms nitric oxide in the vessels. But, when BH_4 is not present, eNOS generates O_2^- and H_2O_2.

Mitochondrial oxidases involve the uncoupling of oxygen during mitochondrial oxidative phosphorylation during the production of ATP to synthesize O_2^-. The superoxide produced during lesion development in the arteries come primarily from the mitochondrial oxidase[12].

In particular, we will analyze more closely the NAD(P)H oxidase as a source of vascular superoxide. NAD(P)H oxidases are present in endothelial cells, fibroblasts, smooth muscle cells, neutrophils, and phagocytic mononuclear cells[2]. The study of NAD(P)H will start at the biochemical reaction of the compound in the cardiovascular system. NAD(P)H is a multi-subunit enzyme that catalyzes O_2^- production by reducing oxygen by one electron and using the NAD(P)H as the electron donor[7].

$$NAD(P)H + 2O_2 \rightarrow NAD(P)^+ + H^+ + 2O_2^- \quad (1)$$

One of the major sources of ROS formation is from the NAD(P)H oxidases. Endothelial cells and fibroblasts express both NAD(P)H oxidase 2 (Nox2) and NAD(P)H oxidase 4 (Nox4). Vascular smooth muscle cells express Nox1 and Nox4[4].

In addition, nitric oxide released by endothelial cells is a key chemical that regulates blood flow. In oxidative stress conditions the availability of nitric oxides is reduced in vascular tissues, which is known as endothelial cell dysfunction. Figure 1 outlines the dysfunction in endothelial cell[4].

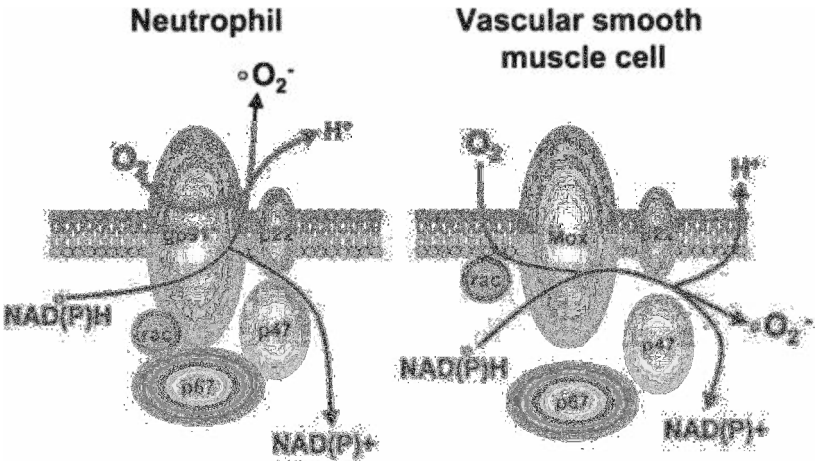

Figure 1: Dysfunction in Endothelial Cell. The following diagram demonstrates how NAD(P)H catalyzes superoxide production by becoming the electron receptor for Oxygen[4].

With this dysfunction comes the natural response of the human body to overcome this production of superoxide. Superoxide is neutralized by a group of antioxidant enzymes. These enzymes include SOD, CAT, GPx, and thiol-disulfide oxidoreductases[12].

This thesis will deal primarily with SOD as the main antioxidant enzyme. There have been three isoforms of SOD identified: mitochondrial manganese-containing SOD (MnSOD, SOD2), the cytosolic copper/zinc-containing SOD (CuZnSOD, SOD1) and the extracellular SOD (eSOD, SOD3)[13]. SOD dismutase superoxide to from hydrogen peroxide and oxygen.

Loss of endothelial NO available to endothelial cells is caused by the reaction with O_2^-. This reaction forms $ONOO^-$, which is a key component in many cardiovascular diseases such as hypertension, diabetes, and atherosclerosis. Understanding the levels of nitric oxide, superoxide, and peroxynitrite will cause a better understanding of the diseases and the oxidative stress state of the vascular system.

A mathematical model was created by Kavdia and Popel in 2004, that created the concentration profiles for NO, $ONOO^-$, and O_2^- for an arterial and venule pair during microcirculation[1]. This model defines the geometry of the arterial and venule vessels parallel to each other, while using diffusion rates and chemical reaction rates to calculate the concentration profiles.

The objective of this thesis is to predict NO, $ONOO^-$, and O_2^- concentration profiles for three different cases: 1) Basal conditions compared to NAD(P)H stimulated conditions (2) Basal conditions in normotensive and hypertensive rats with inactivation of SOD by DETCA (3) NAD(P)H stimulation in normotensive and hypertensive rats with inactivation of SOD by DETCA . For this purpose, we used data from Tamara Paravicini's "Increased NADPH-Oxidase Activity and Nox4 Expression during Chronic Hypertension is Associated with Enhanced Cerebral Vasodilatation to NADPH In Vivo" [3]. In this article the arteries from Wistar-Kyoto rats (WKY) were compared to spontaneously hypertensive rats (SHR). The O_2^- production in these arteries was measured by 5 µmol/L lucigenin-enhanced chemiluminescence under various conditions. The results from Paravicini's experiment are in Figure 2. The trends in this data were applied to the Kavdia and Popel model for the purpose of my thesis.

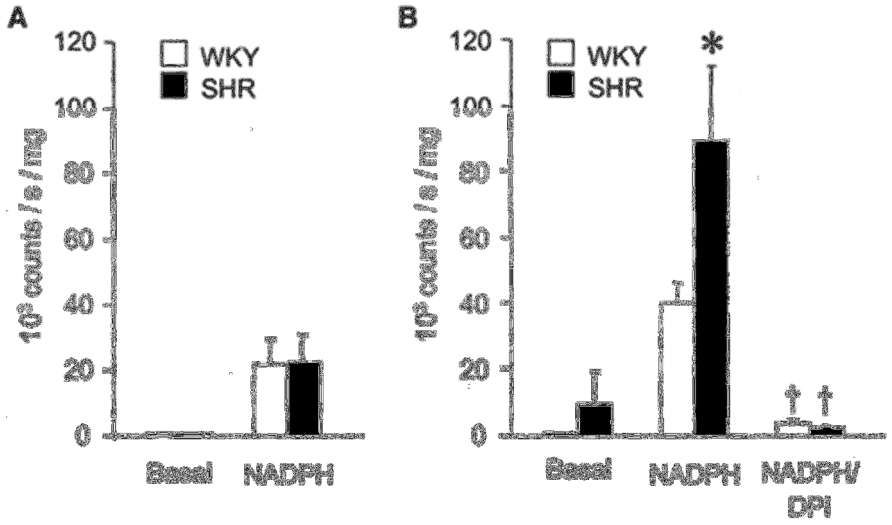

Figure 2. Effect of NADPH on $O_2^{\cdot-}$ production in basilar arteries from WKY and SHR in the absence (a) and presence (b) of DETCA (3 mmol/L) to inactivate Cu^{2+}/Zn^{2+}-SOD. Vascular $O_2^{\cdot-}$ was measured with the use of lucigenin-enhanced chemiluminescence; values are expressed as 10^3 counts per second per milligram dry tissue weight. **P*<0.05 vs similarly treated WKY rings[3].

Methods

Model Geometry:

A previous model by Kavdia and Popel is used to simulate arteriole/venule during microcirculation. This model contains six different regions in the vessels: red blood cell rich (CR), red blood cell free (CF), endothelium (E), interstitial space (IS), smooth muscle (SM), and a nonperfused parenchymal tissue (NPT). The parenchymal tissue (PT) is the region around the arteriole and venule pair. Figure 3 shows the arterial and venule vessel next to each other. The regions have increasing diameters for each separate layer. Nitric Oxide (NO) is produced at the luminal and abluminal surfaces of the endothelium[10].

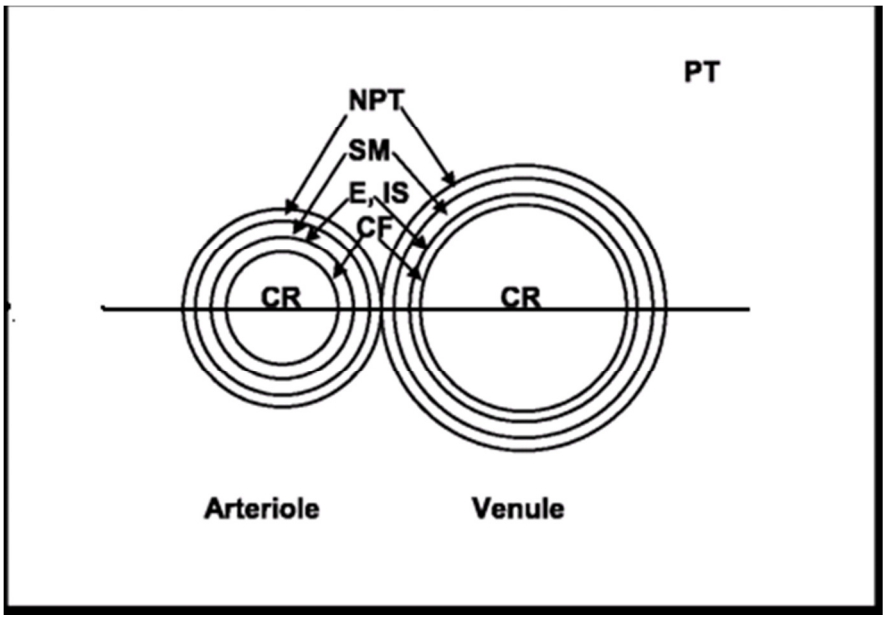

Figure 3: Model Geometry of the arterial and venule vessel from Kavdia and Popel[1].

The steady-state mass transport equation (cylindrical conditions) can be used to solve for the NO mass transport because of the convective transport of NO can be neglected and the NO profiles reach steady state within milliseconds[10].

$$D_j \nabla^2 C_j \pm \sum R_{j,i} = 0 \qquad (2)$$

Where j represents the particular model of interest; C_j is the concentration; D_j is the diffusivity; and $R_{j,i}$ stands for the production and consumption of the species due to chemical reactions.

Boundary Conditions:

Specific boundary conditions will need to be set to model this geometry and diffusion rates. At the outer edge of the PT, a zero-flux boundary condition was fixed, and at the interfaces with the endothelium, the release of NO and O_2^- were given by the following equations respectfully[10].

$$Q_j = D_j \frac{\partial C_{j,en}}{\partial r} - D_j \frac{\partial C_{j,is}}{\partial r} \quad (3)$$

$$Q_j = D_j \frac{\partial C_{j,cf}}{\partial r} - D_j \frac{\partial C_{j,en}}{\partial r} \quad (4)$$

We will obtain NO and O_2^- concentration profiles in the vascular tissue from these equations.

Chemical Reactions:

The chemical reactions that are involved in the different layers of the arterial and venule are a mixture of first and second order reactions. Each region is discusses in further detail in Kavdia's "Venular endothelium-derived NO can affect paired arteriole: a computational model"[14]. The areas that are rich in red blood cells contain high levels of hemoglobin. This hemoglobin reacts at a high rate with the NO in the region.

$$R_{NO,CR} = K_{CR}C_{NO} \quad (5)$$

Where k_{CR} is the effective NO reaction rate constant. All these values can be found in Table 1.

In the CF region the chemical reactions are first order reactions because the hematocrit in this region is assumed to be zero[10].

$$R_{NO,CR} = k_{CF}C_{NO} \quad (6)$$

In the remaining of the regions E, IS, and NPT the NO reaction is a second order reaction[10].

$$R_{NO,\,I} = k_{o2}C^2_{NO}C_{O2} \quad (7)$$

Vascular smooth muscle sGC consumes the NO for the smooth muscle region (SM)[10] . Therefore the second-order reaction is:

$$R_{NO} = k_{SM}\,C^2_{NO} \quad (8)$$

For the capillary-perfused PT region, the endothelial cells of the capillaries produce NO. For this region the reaction rate will have to take in account the amount of nitric oxide that is released by the capillary endothelial cell.

$$R_{NO} = k_{cap}C_{NO}\text{-}Q_{cap} \quad (9)$$

Each region is different, so each individual chemical reaction must be considered when deriving the model.

Parameter Values:

All parameters that were defined in the previous equations used in the model can be found in Table 1. The geometry of the arterial and venule vessels was discussed in previous reports[1]. The venule is assumed to be twice the size of the arteriole. The arteriole is 25 μm and the venule is 50

μm in diameter. This ratio was assumed due to the reported distance between the arteriole and venule vessels[15]. The diffusivity rates of NO, O_2^-, and peroxynitrite are assumed to be constant across the geometry and equal 3.3 x 10^{-5}, 2.8 x 10^{-5}, and 2.6x 10^{-5} cm^2/s respectively according to Table 1. To determine the consumption of NO in CR region, Kavdia and Popel used a hematocrit of 0.45 in the region[1]. The reaction rate for the consumption of NO is 1,270 s^{-1} in the region[9]. The NO that is released by the capillary endothelial cell, k_{cap} can be determined using a hematocrit of 0.3 and a capillary volume of 0.0146 cm^3 for the model [10] . The k_{cap} calculated was 12.4 s^{-1} for this case[16].

Numerical Solutions:

Flex PDE 3.0 software was used for modeling the arteriolar and venular endothelial NO, O_2^-, and $ONOO^-$ concentrations. Flex PDE 3.0 is computer software that can be used for modeling and solving numerical problems.

Simulations:

Tamara M. Paravicini's article "Increased NADPH-Oxidase Activity and Nox4 Expression during Chronic Hypertension is Associated with Enhanced Cerebral Vasodilatation to NADPH In Vivo" showed us experimental trends in the production of superoxide (O_2^-) in Wistar-Kyoto rats (WKY) and Spontaneously Hypertensive rats (SHR). This data was assumed for a model of the human arterial/venule microcirculation during normotension and hypertension. For the base case we used the whole tissue superoxide production as fraction c = 0.2 of NO production and used 10 μM of SOD.

The first simulation involved an increase of O_2^- production by 22-fold due to the NADPH stimulation of the arteriolar and venule. For this case the new whole tissue superoxide production

fraction of NO production was c = 4.4 The SOD remained at 10μM. The results of both the normotensive and hypertensive were compared for basal and NADPH stimulated vessels.

The second simulation compared the three different basal conditions with a difference in the level of SOD. We used a condition with SOD of 10μM and a superoxide production fraction c = 0.2 and compare it to the normotensive and hypertensive basal condition with an inactivation of SOD. The experiment used Cu^{2+} chelating agent diethyldithiocarbamic acid trihydrate (DETCA) to inactive the Cu^{2+}/Zn^{2+} SOD. We assumed that SOD was reduced and the level was assumed to change from 10μM to 1μM. In normotensive basal condition with reduction of SOD the superoxide production fraction remained at c = 0.2, but for hypertensive basal conditions the superoxide production fraction was c = 2 due to a 10-fold increase in superoxide production.

The third simulation compared the NAD(P)H stimulated hypertensive/normotensive vessels with the change in SOD. With SOD of 10 μM, the normotensive and hypertensive vessels both had a superoxide production fraction of c = 4.4, which are 22-fold greater than the basal conditions. With DETCA reduction of SOD to 1 μM, the normotensive vessels had a superoxide production fraction of c = 8, which was a 40-fold increase from the basal conditions. With DETCA reduction of SOD to 1 μM, the hypertensive vessels had a superoxide production fraction of c = 18.4, which was 2.3-fold greater than the normotensive NADPH stimulated conditions.

Results

Normotensive and Hypertensive Cases (Basal and NADPH excited) with SOD of 10µM: Profiles for the reactive oxidative species were generated according to the concentration values along the horizontal center axis of the geometry, as seen in Figure 3. The very first vertical line on the graph at 0.975 cm represented the middle of the arterial vessel. The endothelial cell region was 5 µm, therefore the second line was hard to distinguish from the first because it was at 0.9775 cm on the graph. The third vertical line represented the smooth muscle cell region in the arterial vessel. The fourth vertical line represented the middle of the venule vessel at 0.105 cm on the graph. For the base case, we used normal parameters as described in the methods section. The plots of NO, O_2^-, and $ONOO^-$ concentrations for the base case are displayed in Figures 4, 5 and 6, respectively. As you can see in Figure 4, the NO production of the Basal hypertensive and Basal normotensive with SOD of 10 µM is the same. This simulation of basal hypertensive and normostenive with SOD of 10 µM had the highest NO concentration and the lowest O_2^- concentration. The NAD(P)H stimulated hypertensive and normotensive with SOD of 10 µM were equal to each other. The NO concentration in the lumen of the CR region of both the arterial and venule was zero. As the NO profile approached the EN region the concentration reaches 100 nM. From that region, the NO concentration profile decreased back to 0 nM in the lumen of the venule vessel. The NAD(P)H stimulation during this case only caused a noticeable change in the NO profile in the PT region surrounding the arterial and venule pair.

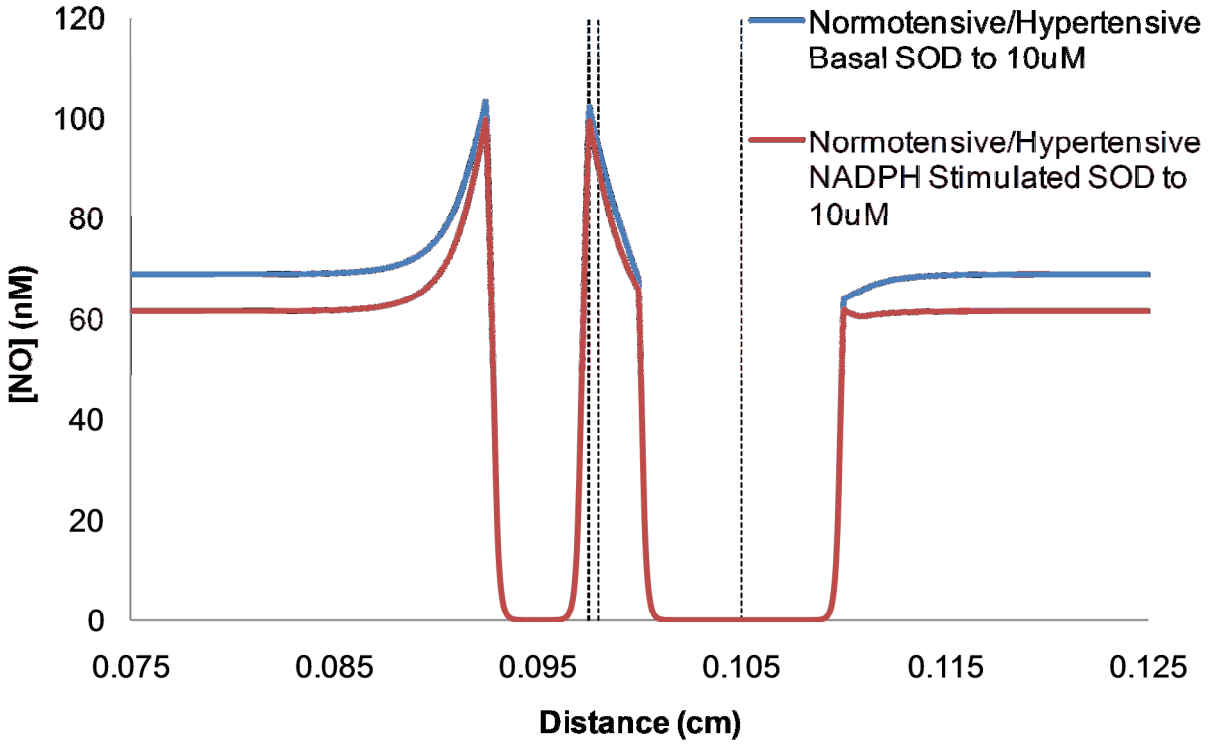

Figure 4: Nitric oxide (NO) concentration profile shown for a 50 µm diameter arteriole and a 100 µm diameter venule. This graph represents the NO for normotensive and hypertensive vessels under Basal and NADPH stimulated conditions with an SOD level of 10µM. The concentration profile is modeled about the horizontal axis in Figure 3.

The $ONOO^-$ concentration profile showed a visible change in Figure 5 throughout the arterial and venule pair due to the NAD(P)H stimulation. This stimulation caused a 20-fold increase in the $ONOO^-$ concentration. In the SM region, the $ONOO^-$ concentration increased from 1 nM to 2.5 nM due to the NAD(P)H stimulation. The perioxynitrite concentration was 0 nM in the lumen of the venule vessel.

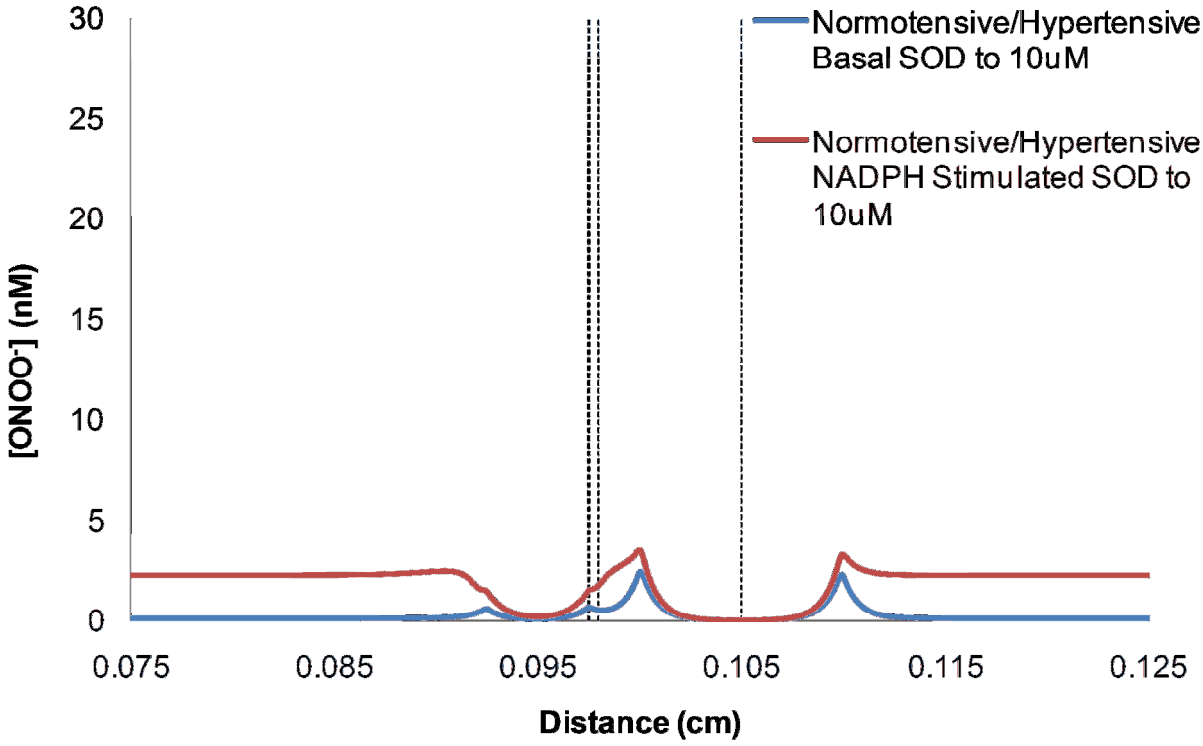

Figure 5: Peroxynitrite [$ONOO^-$] concentration profile shown for a 50 µm diameter arteriole and 100 µm diameter venule vessel. This graph represents the $ONOO^-$ for normotensive and hypertensive vessels under Basal and NADPH stimulated conditions with an SOD level of 10µM. The concentration profile is modeled about the horizontal axis in Figure 3.

The O_2^- concentration profile is in Figure 6. This concentration profile shows that there was an increase in superoxide production in both the arterial and venule EN region. The O_2^- concentration had a peak at 0.433 nM and 2.29 nM in the arterial EN and venule EN, respectively.

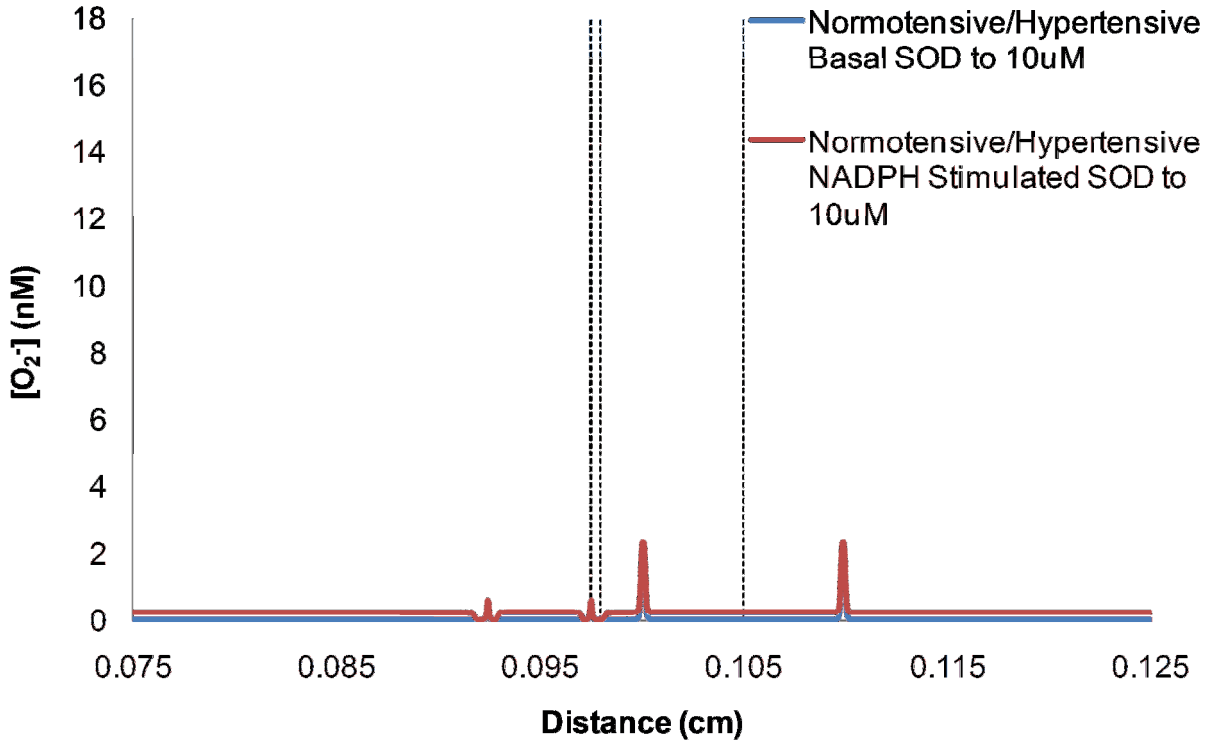

Figure 6: Superoxide (O_2^-) concentration profile shown for a 50 µm diameter arteriole and 100 µm diameter venule vessel. This graph represents the O_2^- for normotensive and hypertensive vessels under Basal and NADPH stimulated conditions with an SOD level of 10µM. The concentration profile is modeled about the horizontal axis in Figure 3.

Normotensive and Hypertensive Cases (Basal Only) with SOD being inactivated from 10 µM to 1 µM: We modeled the concentration profile of NO, $ONOO^-$, and O_2^- for the basal case only of normotensive and hypertensive cases, but the SOD was reduced from 10µM to 1 µM with DETCA Cu^{2+}/Zn^{2+}. The nitric oxide production in the reduced SOD was lower than that of the 10 µM SOD cases. Also the NO level for hypertensive case with SOD of 1 µM was much lower than the normotensive case with SOD of 1µM under basal conditions. Figure 7 shows the highest concentrations of the NO was 102.3 nM, 96.1nM, and 89.05 nM for Normotensive/Hypertensive

basal case with SOD to 10 µM, Normotensive basal case SOD to 1 µM, and Hypertensive basal case with SOD to 1 µM, respectively in the EN arterial regions. The hypertensive basal case with SOD to 1 µM shows a NO concentration that was 20 nM less in the PT surrounding region of the arterial/venule pair compared to normotensive vessels in the same case.

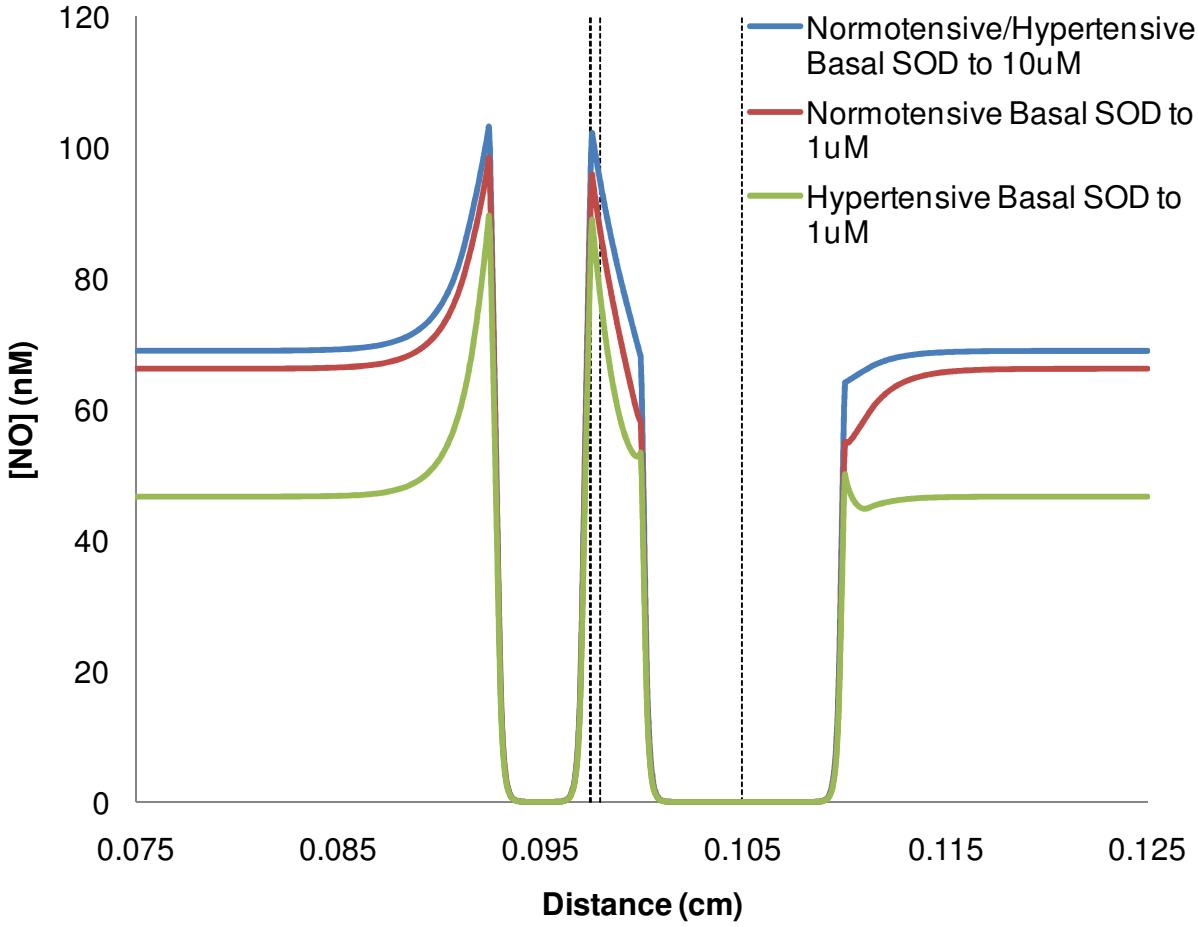

Figure 7: Nitric oxide (NO) concentration profile shown for a 50 µm diameter arteriole and 100 µm diameter venule vessel. This graph represents the NO concentrations for normotensive and hypertensive vessels under Basal conditions with an SOD level changing from 10µM to 1µM. The concentration profile is modeled about the horizontal axis in Figure 3.

The peroxynitrite concentration profile is shown in Figure 8. The hypertensive vessel with SOD reduction to 1 µM had the highest levels of $ONOO^-$. This corresponds to the same case having the lowest levels of NO. The peak in the arterial vessel was in the EN and SM region. The concentration levels were 6.56 nM, 4.25 nM, and 0.647 nM in hypertensive basal case with SOD to 1 µM, normotensive basal case with SOD to 1 µM, and normotensive/hypertensive basal case with SOD to 10 µM, respectively. The peaks for the venule EN and SM region were 17.8 nM, 15.6 nM, and 2.36 nM, respectively.

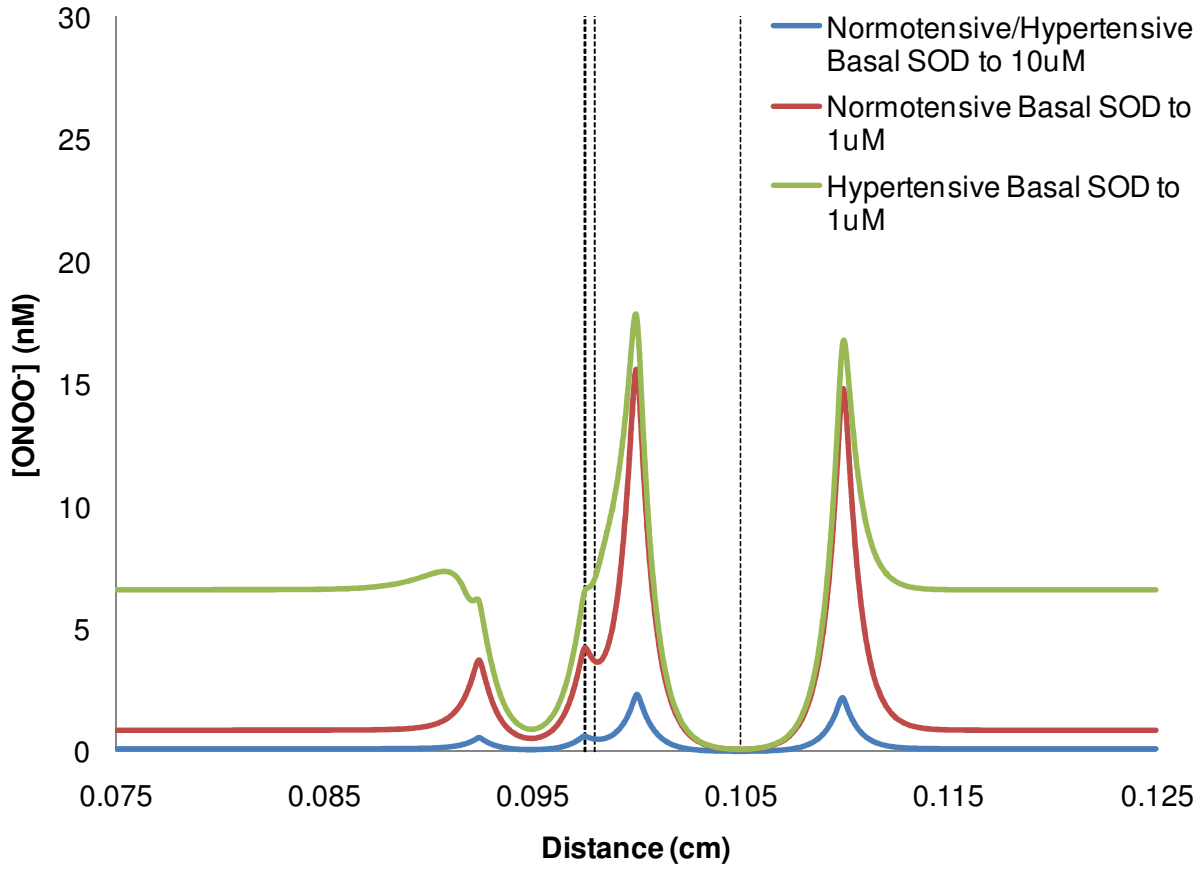

Figure 8: Peroxynitrite [$ONOO^-$] concentration profile shown for a 50 µm diameter arteriole and 100 µm diameter venule vessel. This graph represents the $ONOO^-$ concentrations for normotensive and hypertensive vessels under Basal conditions with an SOD level changing from 10µM to 1µM. The concentration profile is modeled about the horizontal axis in Figure 3.

The superoxide concentration profiles for these specific cases are in Figure 9. This profile shows us that the SOD reduction caused an increase of superoxide in the vessels by 10-fold in hypertensive vessels compared to the cases with SOD of 10 µM. In the hypertensive basal case with SOD reduced, the superoxide concentration was 1.81 nM and 13.3 nM in arterial and venule EN region, respectively. In comparison the arterial and venule EN region of normotensive basal with an SOD level of 1 µM had peaks of 1.54 nM and 12.83 nM, respectively.

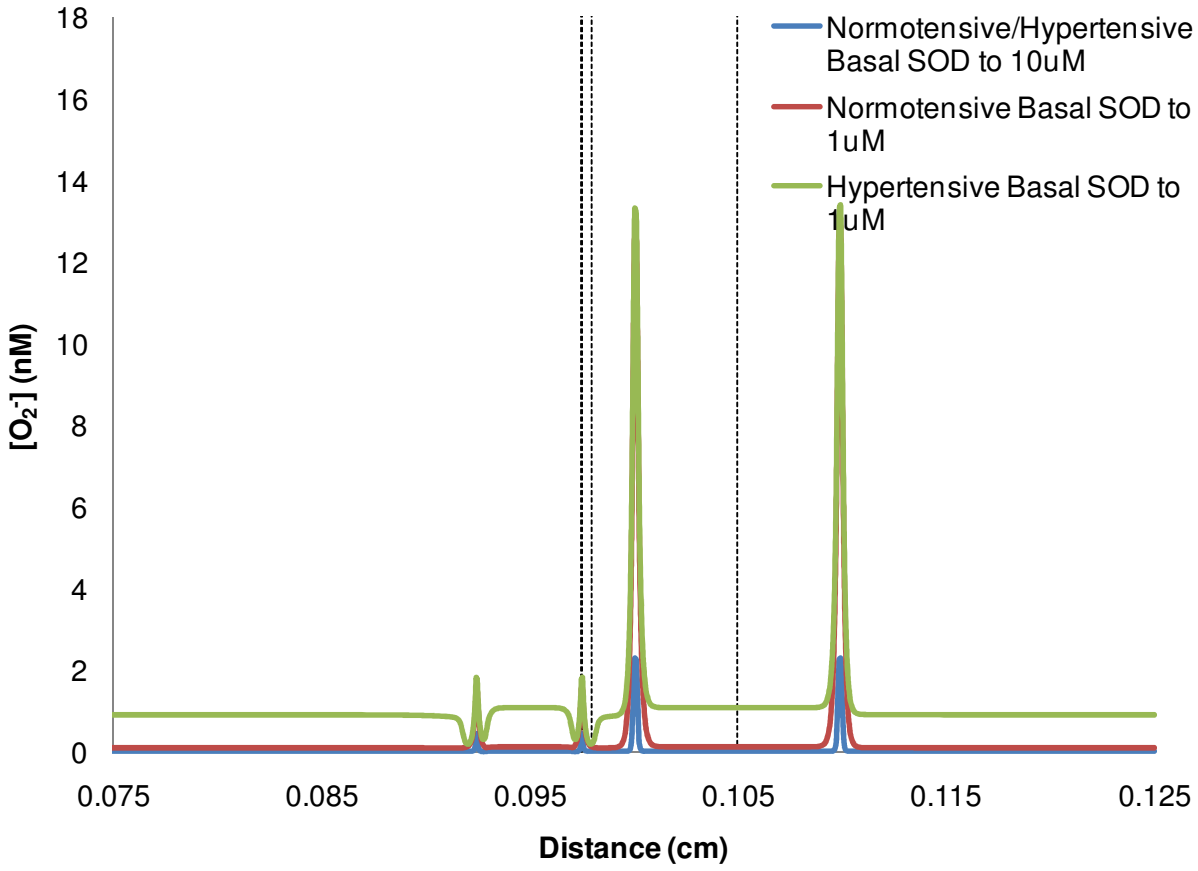

Figure 9: Superoxide (O_2^-) concentration profile shown for a 50 µm diameter arteriole and 100 µm diameter venule vessel. This graph represents the O_2^- concentrations for normotensive and hypertensive vessels under Basal conditions with an SOD level changing from 10µM to 1µM. The concentration profile is modeled about the horizontal axis in Figure 3.

Normotensive and Hypertensive Cases (NADPH excited) with SOD being inactivated from 10 µM to 1 µM: Finally the profile for the NO, $ONOO^-$, and O_2^- for normotensive and hypertensive vessels under NAD(P)H excited conditions with SOD reduced from 10 µM to 1µM. The hypertensive NAD(P)H excited vessels with an SOD of 1 µM had the lowest concentration of nitric oxide. These results are shown in Figure 10. The endothelial region of the arterial vessel had the highest concentration of NO during microcirculation. During normotensive/hypertensive vessels with NAD(P)H stimulation and with SOD of 10 µM, the concentration was 99.6 nM. But when SOD is reduced to 1 µM, the NO concentration in normotensive was75.6 nM and in hypertensive was 65.2 nM. The lumen of both the arterial/venule pair was reduced to 0 nM in all three cases.

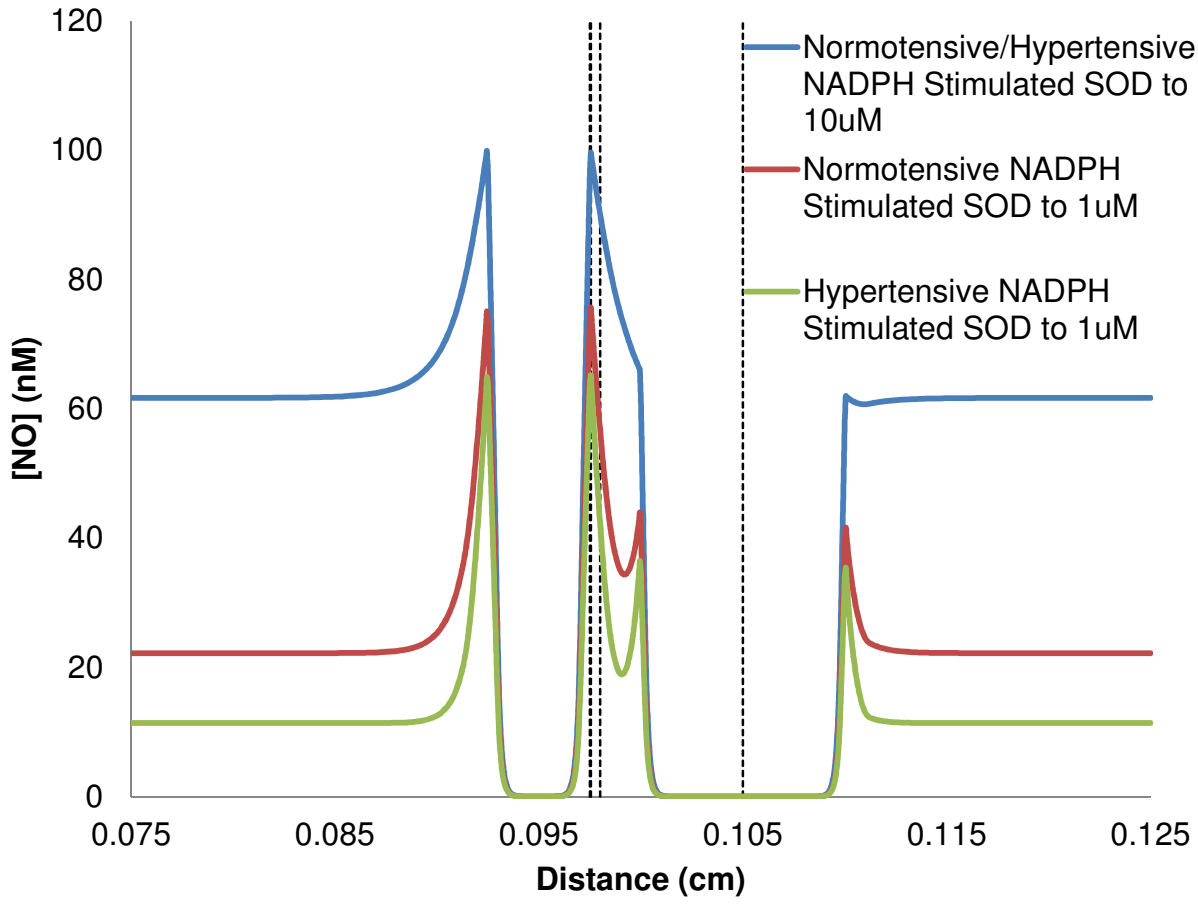

Figure 10: Nitric oxide (NO) concentration profile shown for a 50 µm diameter arteriole and 100 µm diameter venule vessel. This graph represents the NO concentrations for normotensive and hypertensive vessels under NAD(P)H stimulated conditions with an SOD level changing from 10µM to 1µM. The concentration profile is modeled about the horizontal axis in Figure 3.

The $ONOO^-$ concentration profile for the NAD(P)H cases with SOD reduction are presented in Figure 11. The reduced SOD, hypertensive vessels had the highest $ONOO^-$ concentrations. The lowest concentrations of perioxynitrite were in the lumen of the venule. The highest concentrations of the ONOO- were in the EN and SM region of the venule vessel. The concentrations were 29.4 nM, 23.3 nM, and 3.45 nM for the reduced SOD hypertensive, reduced SOD normotensive, and the 10 µM SOD normotensive/hypertensive, respectively.

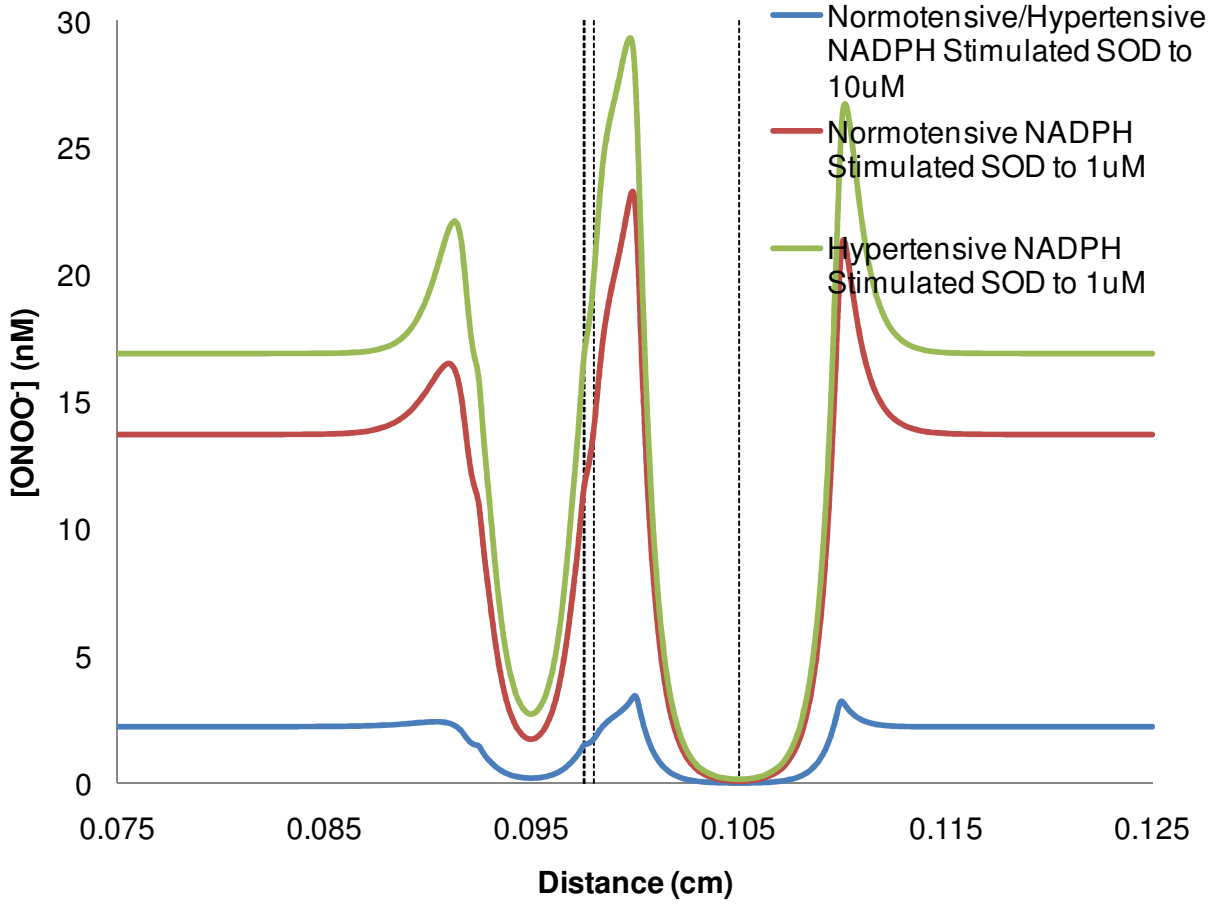

Figure 11: Peroxynitrite [$ONOO^-$] concentration profile shown for a 50 µm diameter arteriole and 100 µm diameter venule vessel. This graph represents the $ONOO^-$ concentrations for normotensive and hypertensive vessels under NAD(P)H stimulated conditions with an SOD level changing from 10µM to 1µM. The concentration profile is modeled about the horizontal axis in Figure 3.

The superoxide concentration profile for the NAD(P)H cases is shown in Figure 12. This profile shows that when the SOD was reduced in the hypertensive vessels the O_2^- concentration peaks in the EN and SM of both the arterial and venule vessels. The arterial EN concentration level was lower than that of the venule because in the arterial the superoxide levels dropped dramatically before these regions. In hypertensive vessels with SOD reduction, the arterial EN superoxide concentration was 4.4 nM and in the venule EN superoxide concentration was 17.5 nM. In normotensive vessels with SOD reduction, the arterial EN superoxide concentration was 2.9 nM and in the venule EN superoxide concentration was 14.9 nM.

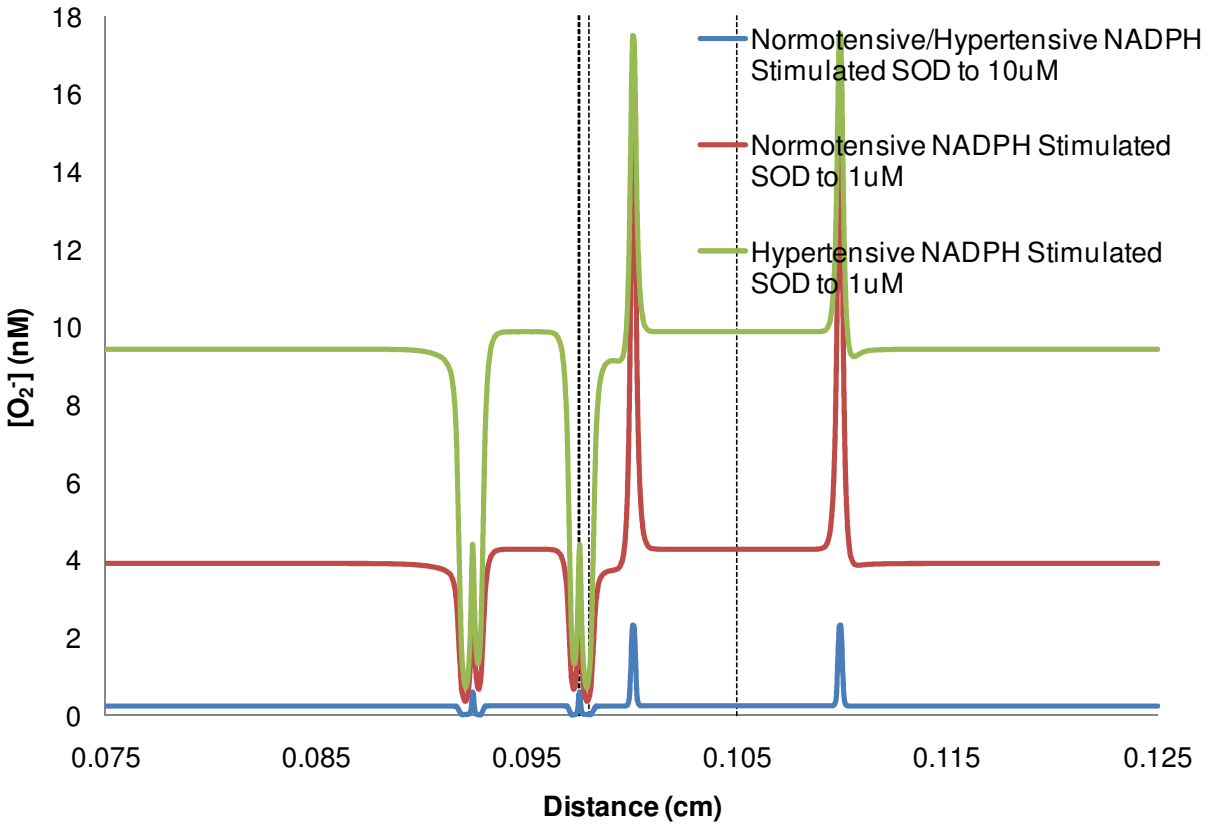

Figure 12: Superoxide (O_2^-) concentration profile shown for a 50 µm diameter arteriole and 100 µm diameter venule vessel. This graph represents the O_2^- concentrations for normotensive and hypertensive vessels under NAD(P)H stimulated conditions with an SOD level changing from 10µM to 1µM. The concentration profile is modeled about the horizontal axis in Figure 3.

Discussion

Effects of SOD Inactivation: SOD inactivation can be shown to increase the superoxide production by 10-fold in Basal Hypertensive cases. This results in an increase in peroxynitrite but a decrease in the nitric oxide. SOD reduction with NAD(P)H stimulation caused an increase of 2.1-fold and 4.1-fold in superoxide production in normotensive and hypertensive vessels, respectively when compared to vessels with SOD of 10 μM. When SOD was activated, the superoxide production was the same in hypertensive and normotensive vessels. This shows that SOD is very important in controlling O_2^- production and also vascular disease. Without SOD, the level of superoxide may increase dramatically inducing vascular diseases When SOD is 10 μM, the vessels have a higher than normal level of H_2O_2 due to the dismutase of superoxide. This explains why the levels of H_2O_2 in plasma is higher than normotensive patients[3]. This level of H_2O_2 which is a powerful vasodilator, may have important consequences in the vascular system [3]. The current therapies for vascular disease, such as β-blockers, angiotensin antagonists, and angiotensin-converting enzyme inhibitors, act like antioxidants in some way[17]. New antioxidant therapies have the potential to be discovered to treat hypertension.

Effects of Normotension vs. Hypertension:

Spontaneous hyptertensive vessels can cause a 10-fold increase from normotensive vessels in basal conditions and a 2.3-fold increase from normotensive vessels in NAD(P)H stimulated vessels. This data shows that superoxide production is increased dramatically in hypertensive vessels. In hypertensive basilar vessels the Nox4 was 4.1-fold higher[3]. This shows that there is a direct correlation of the increase of NAD(P)H oxidase in regions with the increase of production with superoxide and vasodilation. In the area directly before the EN region the superoxide level

decreases dramatically. But, it can be seen that in the endothelial region there is a large increase in superoxide production. This can be explained because this is where Nox4 is found to be most prevalent. Nox4 mRNA is seen to be 125 -fold higher in endothelial cells than in smooth muscle cells [2].

(x10^5/10^9 copies 18S)	Gp91phox	Nox4	Nox1	p22phox
Monocyte	6140	Undetectable	0.10	447
Endothelial cells	13.2	270.0	0.87	45.8
Smooth Muscle Cells	0.19	2.15	0.22	81.6
Fibroblasts	0.58	6.25	0.45	10.9

Table 2: Real-time PCR quantified the levels of RNA expression of Nox isoforms from cultured human cells. Values are expressed as copy numbers per 10^9 copies of 18S measured in the same sample [2].

Also Nox4 and Nox1 mRNA levels are 2.5-fold and 10-fold greater in spontaneously hypertensive rats than in age-matched Wistar Kyoto rats, respectively [18]. This data that was published and the results from this model, showed a direct corrlation between superoxide production and Nox expression.

Effects of NAD(P)H stimulation:

When NAD(P)H was used to stimulate the vessels, it increased superoxide in the cells because the NAD(P)H is reacted with the oxygen in the vessels. During this reaction, superoxide was produced, which significantly increased the levels of superoxide in the vessels. NAD(P)H stimulation increased the superoxide produce 22-fold compared to normal basal conditions when

SOD was 10 μM. During NAD(P)H stimulation when SOD was reduced to 1 μM, the superoxide production was 40-fold higher and 92-fold higher of normotensive and hypertensive, respectively when compared to normal basal conditons. In human coronary arteries, NAD(P)H stimulation is the major source of superoxide production and in human coronary artery disease the NAD(P)H acivity is significantly increased[5].

Importance and Conclusion:

The importance of this model was to provide insight for oxidative stress in hypertension. During hypertension there is proven to be an increase in superoxide production is increased when SOD is decreased. The trends from the NO, $ONOO^-$, and O_2^- concentration profile show us which regions are affected by the disease and the physiological affects on the walls of the arteriole and venule. Also, the H_2O_2 generated during superoxide dismutase may have a signifcant correlation to the vasodilation during hypertension. The relevance of this thesis is underlined in the major role of oxidative stress in vascular diseases. The future of cardiovascular therapy is based on the balance between NO, $ONOO^-$, and O_2^- within the body [19].

Future Work:

The data from this thesis can be used to further progress the understanding of vascular diseases. Nox1 and Nox4 are highest in the endothelial and smooth muscle cell region. The NAD(P)H oxidases are also proven to be expressed more in hypertension during normotension. As previously stated the expression of Nox1 is 10-fold greater and Nox4 is 2.5-fold greater. Most recently, there have been papers published that treats the arterioles and veins with different medication. Very similar tests were done to measure superoxide production and Nox expression.

In one particular experiment, the vessels were treated with different hypertension medications: 1) high dose candesartan 2) low dose of candesartan 3) a dose of a combined hyralazine and hydrochlorothiazide [18]. All three treatments reduced the expression of Nox1 and Nox4. From the data from this experiment the reduction of Nox1 and Nox4 can also be hypothesized to reduce the superoxide levels produce in the arterial and venule flow. The data shows the strong correlation might suggest a stronger link between NAD(P)H stimulation and the development of vascular diseases. In future research, we would model the concentration profiles of medically treated vessels.

References

1. Kavdia M, Popel AS. Contribution of nNOS- and eNOS-derived NO to microvascular smooth muscle NO exposure. *J Appl Physiol.* 2004;97(1):293-301.

2. Sorescu D, Weiss D, Lassegue B, Clempus RE, Szocs K, Sorescu GP, Valppu L, Quinn MT, Lambeth JD, Vega JD, Taylor WR, Griendling KK. Superoxide production and expression of nox family proteins in human atherosclerosis. *Circulation.* 2002;105(12):1429-1435.

3. Paravicini TM, Chrissobolis S, Drummond GR, Sobey CG. Increased NADPH-oxidase activity and Nox4 expression during chronic hypertension is associated with enhanced cerebral vasodilatation to NADPH in vivo. *Stroke.* 2004;35(2):584-589.

4. Griendling KK, Sorescu D, Ushio-Fukai M. NAD(P)H oxidase: role in cardiovascular biology and disease. *Circ Res.* 2000;86(5):494-501.

5. Guzik TJ, Sadowski J, Guzik B, Jopek A, Kapelak B, Przybylowski P, Wierzbicki K, Korbut R, Harrison DG, Channon KM. Coronary artery superoxide production and nox isoform expression in human coronary artery disease. *Arterioscler Thromb Vasc Biol.* 2006;26(2):333-339.

6. Yamashita T, Shoge M, Oda E, Yamamoto Y, Giddings JC, Kashiwagi S, Suematsu M, Yamamoto J. The free-radical scavenger, edaravone, augments NO release from vascular cells and platelets after laser-induced, acute endothelial injury in vivo. *Platelets.* 2006;17(3):201-206.

7. Touyz RM, Schiffrin EL. Reactive oxygen species in vascular biology: implications in hypertension. *Histochem Cell Biol.* 2004;122(4):339-352.

8. Szasz T, Thakali K, Fink GD, Watts SW. A comparison of arteries and veins in oxidative stress: producers, destroyers, function, and disease. *Exp Biol Med (Maywood).* 2007;232(1):27-37.

9. Kavdia M, Popel AS. Wall shear stress differentially affects NO level in arterioles for volume expanders and Hb-based O2 carriers. *Microvasc Res.* 2003;66(1):49-58.

10. Kavdia M. A computational model for free radicals transport in the microcirculation. *Antioxid Redox Signal.* 2006;8(7-8):1103-1111.

11. Guzik TJ, Mussa S, Gastaldi D, Sadowski J, Ratnatunga C, Pillai R, Channon KM. Mechanisms of increased vascular superoxide production in human diabetes mellitus: role of NAD(P)H oxidase and endothelial nitric oxide synthase. *Circulation.* 2002;105(14):1656-1662.

12. Bonomini F, Tengattini S, Fabiano A, Bianchi R, Rezzani R. Atherosclerosis and oxidative stress. *Histol Histopathol.* 2008;23(3):381-390.

13. Hamilton CA, Miller WH, Al-Benna S, Brosnan MJ, Drummond RD, McBride MW, Dominiczak AF. Strategies to reduce oxidative stress in cardiovascular disease. *Clin Sci (Lond).* 2004;106(3):219-234.

14. Kavdia M, Popel AS. Venular endothelium-derived NO can affect paired arteriole: a computational model. *Am J Physiol Heart Circ Physiol.* 2006;290(2):H716-723.

15. Boegehold MA. Shear-dependent release of venular nitric oxide: effect on arteriolar tone in rat striated muscle. *Am J Physiol.* 1996;271(2 Pt 2):H387-395.

16. Ellsworth ML, Popel AS, Pittman RN. Assessment and impact of heterogeneities of convective oxygen transport parameters in capillaries of striated muscle: experimental and theoretical. *Microvasc Res.* 1988;35(3):341-362.

17. Zhang M, Shah AM. Role of reactive oxygen species in myocardial remodeling. *Curr Heart Fail Rep.* 2007;4(1):26-30.

18. Akasaki T, Ohya Y, Kuroda J, Eto K, Abe I, Sumimoto H, Iida M. Increased expression of gp91phox homologues of NAD(P)H oxidase in the aortic media during chronic hypertension: involvement of the renin-angiotensin system. *Hypertens Res.* 2006;29(10):813-820.

19. Kalinowski L, Malinski T. Endothelial NADH/NADPH-dependent enzymatic sources of superoxide production: relationship to endothelial dysfunction. *Acta Biochim Pol.* 2004;51(2):459-469.
20. Haas TL, Duling BR. Morphology favors an endothelial cell pathway for longitudinal conduction within arterioles. *Microvasc Res.* 1997;53(2):113-120.
21. Popel AS. Theory of oxygen transport to tissue. *Crit Rev Biomed Eng.* 1989;17(3):257-321.
22. Buerk DG, Lamkin-Kennard K, Jaron D. Modeling the influence of superoxide dismutase on superoxide and nitric oxide interactions, including reversible inhibition of oxygen consumption. *Free Radic Biol Med.* 2003;34(11):1488-1503.
23. Vaughn MW, Kuo L, Liao JC. Estimation of nitric oxide production and reaction rates in tissue by use of a mathematical model. *Am J Physiol.* 1998;274(6 Pt 2):H2163-2176.
24. Zacharia IG, Deen WM. Diffusivity and solubility of nitric oxide in water and saline. *Ann Biomed Eng.* 2005;33(2):214-222.
25. Nalwaya N, Deen WM. Analysis of cellular exposure to peroxynitrite in suspension cultures. *Chem Res Toxicol.* 2003;16(7):920-932.
26. Lewis RS, Deen WM. Kinetics of the reaction of nitric oxide with oxygen in aqueous solutions. *Chem Res Toxicol.* 1994;7(4):568-574.
27. Huie RE, Padmaja S. The reaction of no with superoxide. *Free Radic Res Commun.* 1993;18(4):195-199.
28. Carlsen E, Comroe JH, Jr. The rate of uptake of carbon monoxide and of nitric oxide by normal human erythrocytes and experimentally produced spherocytes. *J Gen Physiol.* 1958;42(1):83-107.
29. Fridovich I. Superoxide radical and superoxide dismutases. *Annu Rev Biochem.* 1995;64:97-112.
30. Radi R. Peroxynitrite reactions and diffusion in biology. *Chem Res Toxicol.* 1998;11(7):720-721.
31. Pfeiffer S, Gorren AC, Schmidt K, Werner ER, Hansert B, Bohle DS, Mayer B. Metabolic fate of peroxynitrite in aqueous solution. Reaction with nitric oxide and pH-dependent decomposition to nitrite and oxygen in a 2:1 stoichiometry. *J Biol Chem.* 1997;272(6):3465-3470.

Table 1. Model Parameters			
Parameter	*Value*	*Units*	*Reference*
Systemic hematocrit	45	%	[14]
Capillary hematocrit	30	%	[14]
Arteriole radius	25	μm	[14]
RBC-free-layer thickness	4.5	μm	[14]
Endothelium thickness	0.5	μm	
Interstitual Space thickness	0.5	μm	[14]
Smooth Muscle thickness	6	μm	[20]
NPT thickness	30	μm	[10]
O_2 concentration	27	μM	[21]
SOD concentration	1 (0.1)	μM	[22]
CO_2 concentration	1.14(0.114)	mM	
Half NO release rate, Q_{NO}	2.65×10^{-12}	mol $cm^{-2}s^{-1}$	[23]
Half O_2^- release rate, Q_{02}^-	0.2 (2) x Q_{NO}	mol $cm^{-2}s^{-1}$	[14]
D_{NO}	3.3×10^{-5}	cm^2s^{-1}	[24]
D_{02}^-	2.8×10^{-5}	cm^2s^{-1}	[25]
D_{ONOO}^-	2.6×10^{-5}	cm^2s^{-1}	[25]
F(=C_{ONOO}^-/C_{Per}) in tissue	0.640		[14]
F(=C_{ONOO}^-/C_{Per}) in tissue	0.817		[14]
Reaction rates of NO with			
O_2, $-k_{O2}C_{NO}^2C_{O2}$	9.6×10^6	$M^{-2}s^{-1}$	[26]
O_2^-, $-k_{Per}C_{NO}C_{O2}^-$	6.7 (16) x 10^9	$M^{-1}s^{-1}$	[27]
sGC, $-k_{sm}C_{NO}^2$	5×10^4	$M^{-1}s^{-1}$	[23]
RBC	1.4×10^5	$M^{-1}s^{-1}$	[28]
RBC-rch core (CR), $-k_{CR}C_{NO}$	1,270	s^{-1}	[14]
Capillaries, $-k_{cap}C_{NO}+Q_{cap}$	12.4 C_{NO} - 8.6×10^{-7}	s^{-1}	[14]
Reaction rates of O_2^- with			
SOD, $-k_{SOD}C_{O2}^-C_{SOD}$	1.6×10^9	$M^{-1}s^{-1}$	[29]
Reaction rates of $ONOO^-$ with			
CO_2, $-k_{CO2}C_{CO2}fC_{Per}$	5.6×10^4	$M^{-1}s^{-1}$	[30]
NO, $-k_{NO}C_{NO}fC_{Per}$	9.1×10^4	$M^{-1}s^{-1}$	[31]